PCCP

Accepted Manuscript

ROYAL SOCIETY OF CHEMISTRY

www.rsc.org/pccp

Physical Chemistry Chemical Physics

Dynamic Article Links ►

Cite this: DOI: 10.1039/c0xx00000x

www.rsc.org/pccp

PAPER

Noble-metal-free BODIPY-cobaloxime photocatalysts for visible-light-driven hydrogen production†

Geng-Geng Luo,*[a] Kai Fang,[a] Ji-Huai Wu,[a] Jing-Cao Dai[a] and Qing-Hua Zhao[a]

Received (in XXX, XXX) Xth XXXXXXXXX 2014, Accepted Xth XXXXXXXXX 2014

First published on the web Xth XXXXXXXXX 2014

DOI: 10.1039/b000000x

In this study a series of supramolecular BODIPY-cobaloxime systems **Co-Bn** (n = 1-4): [{Co(dmgH)$_2$Cl}{4,4-difluoro-8-(4-pyridyl)-1,3,5,7-tetramethyl-4-bora-3a,4a-diaza-*s*-indacene}] (**Co-B1**), [{Co(dmgH)$_2$Cl}{4,4-difluoro-8-(4-pyridyl)-1,3,5,7-tetramethyl-2,6-diiodo-4-bora-3a,4a-diaza-*s*-indacene}] (**Co-B2**), [{Co(dmgH)$_2$Cl}{4,4-difluoro-8-(3-pyridyl)-1,3,5,7-tetramethyl-4-bora-3a,4a-diaza-*s*-indacene}] (**Co-B3**), and [{Co(dmgH)$_2$Cl}{4,4-difluoro-8-(3-pyridyl)-1,3,5,7-tetramethyl-2,6-diiodo-4-bora-3a,4a-diaza-*s*-indacene}] (**Co-B4**) (BODIPY = boron dipyrromethene, dmgH = dimethylglyoxime) have been synthesized by replacing one axial chlorine of cobaloxime moieties with the pyridine residues of BODIPYs, and structural characterization. Absorption spectra show that the optical properties of the BODIPY-cobaloximes are essentially the sum of their constituent components, indicating weak interactions between the cobaloxime units and BODIPY chromophores in the ground state, if any, electronic communications may take place through the intramolecular electron transfer across their orthogonal structures. The possiblity of intramolecular electron transfer is further supported by the results of the density functional theory (DFT) calculations at UB3LYP/LANL2DZ levels on **Co-B2**$^{\cdot-}$ and **Co-B4**$^{\cdot-}$, which show that the highest occupied molecular orbitals (HOMOs) possess predominantly BODIPY character, while the lowest unoccupied molecular orbitals (LUMOs) are located on the cobalt centers. The HOMO→LUMO transition is an electron-transfer process (BODIPY$^{\cdot-}$ radical anions→cobaloxime fragment). In view of the possible occurrence of electron transfer, these noble-metal-free BODIPY-cobaloximes are studied as single-component homogeneous photocatalysts for H_2 generation in aqueous media. Under optimized conditions, the 2,6-diiodo BODIPY-sensitized cobaloxime **Co-B4** that contains a *meta*-pyridyl at the 8-position of BODIPY presents excellent H_2 photoproduction catalytic activity with 85 turnover number (TON), which is comparable to that of its analogue **Co-B2** that has a *para*-pyridyl substitution attached onto 2,6-diiodo BODIPY (TON = 82), but both of noniodinated BODIPY-sensitizer cobaloximes (**Co-B1**, **Co-B3**) result in a complete lack of activity under the same experimental conditions. These results show that the presence of heavy atoms in the core of BODIPY is essential for the catalytic process and reductive quenching pathways (namely, the intramolecular electron transfers from BODIPY$^{\cdot-}$ species to the cobalt centers) for these photocatalytically active systems of **Co-Bn** (n = 2 and 4) are thermodynamically feasible for the hydrogen-evolving reaction.

1. Introduction

Photocatalytic hydrogen evolution from water splitting is regarded as a holy grail of science, being one route to a no-fossil fuel and a potential source of clean and renewable energy to meet the rising global energy.[1] Generally, photoreduction of water into H_2 under visible-light irradiation includes heterogeneous and homogeneous catalytic systems. The development of heterogeneous catalytic systems using semiconductor-based photocatalysts for hydrogen production has been investigated during last three decades.[2] Homogeneous photocatalysts, however, have experienced considerable growth in sense that their chemical and photochemical properties can be understood and tuned on the molecular level. Currently, homogeneous catalytic systems for the proton reduction to molecular hydrogen comprise multiple-component and single-component systems. A catalytic multiple-component system usually contains a photosensitizer, an electron mediator and a proton reduction catalyst in the presence of a sacrificial electron donor. Nevertheless, these systems still need to be improved because many interfacial interactions could affect the photoinduced electron transfer reactions. In contrast with these multi-component systems, development of single-component photocatalysts in which the photosensitizer is chemically coupled to the hydrogen-evolving catalyst through a bridging ligand to generate integrated molecular or supramolecular systems, would benefit since the more desirable electron transfer processes may be achieved by precise tuning of the physical properties and orientation of the molecular components.[3,4] In recent years, a number of single-component

[a]*College of Materials Science and Engineering, Huaqiao University, Xiamen 361021, P. R. China*; *E-mail: ggluo@hqu.edu.cn; Fax: 86-592-6162225*

†Electronic Supplementary Information (ESI) available. Additional calculations and experimental measurements, figures and tables. CCDC reference numbers 1015448-1015453. For ESI and crystallographic data in CIF or other electronic format see DOI:10.1039/b000000x.

supramolecular photocatalysts have been designed and reported to be active for photochemical H_2 production. These systems include Ru-Pt complexes,[5] Ru-Pd complexes,[6] Ru-Rh complexes[7] and Ir-Co complexes.[8] However, molecular components of these reported systems usually require expensive and unsustainable noble metals as the catalysts or photosensitizers. Completely noble-metal-free molecular devices for water splitting with relatively effective catalysts overall turnover numbers (TONs) for hydrogen formation were still limited.[9]

On the other hand, compared with noble-metal ruthenium, iridium and platinum complexes, a wide variety of organic dyes such as xanthene dyes (Eosin Y and Rose Bengal) and rhodamine dyes as photosensitizes have displayed high efficiencies of photocatalytic hydrogen production from water in the homogeneous multiple-component systems.[10] Besides, another conjugated organic molecule boron-dipyrromethene (BODIPY) is targeted as more tunable photosensitizer due to their outstanding optical properties such as high absorption coefficients, excellent chemical and photochemicalstability, high solubility and weak nonradiative decay of the excited state.[11] Additionally, ease of functionalization of BODIPY makes it possible to fine-tune the energy levels of the S_1 and T_1 excited state by attaching heavy atoms directly onto the chromophore. As pointed out by earlier studies, the presence of heavy atoms facilitates intersystem crossing (ISC) and thus production of a long-lived triplet state required for the efficient transfer of electrons to the catalyst.[10b,12] Recent efforts by other groups and our laboratory have focused on developing BODIPY fluorescence sensors based on photoinduced electron transfer (PET) as a transduction mechanism.[13] Very recently, J. Bartelmess et al., reported halogenated BODIPY-cobaloxime complexes for catalytic light-driven hydrogen evolution.[14] They mainly focus on studying the influence of different halogen atoms and a relatively electron-donating methyl substituent on the pyridine linker on photocatalytic hydrogen generation efficiency. Therein, a *para*-pyridyl substitution attached onto 2,6-diiodo BODIPY was characterized and the corresponding BODIPY-sensitizer cobaloxime was studied as a photocatalyst for hydrogen evolution. However, no control experiments were done to optimize the H_2 photocatalysis experiments and the reported TON was relatively low (TON = 10.1). Additionally, no mechanism of hydrogen generation was analyzed. In this paper, four BODIPY-cobaloxime complexes **Co-Bn** (n = 1-4) have been synthesized and systematically studied as single-component homogeneous photocatalytic systems for H_2 production in aqueous media. The hydrogen evolving performance was found to be strongly dependent on many factors, including the medium, sacrificial electron donor, the ratio of solvent/water and pH in the reaction medium, irradiation wavelength, etc. Under the best optimized conditions, 2,6-diiodo BODIPY-sensitized cobaloximes **Co-B2** and **Co-B4** show photocatalytic hydrogen generation efficiency with TONs of 85 and 82, respectively, while noniodinated **Co-B1** and **Co-B3** result in a complete lack of activity. We further compare the efficiency of *para*-pyridyl and *meta*-pyridyl placed on the 8-position of iodinated BODIPYs (**Co-B2** and **Co-B4**), both of which show similar photocatalytic H_2 production efficiencies in the same experimental conditions. The reductive quenching mechanism of hydrogen evolution was given based on the experimental and theoretical results.

2. Result and discussion

2.1. Synthesis

para-pyridyl substituted BODIPY derivatives of **B1-B2** were prepared according to published procedures,[15] and the method was modified and used to synthesize *meta*-pyridyl substituted BODIPYs of **B3-B4** in this study. Starting from **B1-B4**, the corresponding photocatalysts **Co-Bn** (n = 1-4) were synthesized in a straightforward manner by the reaction of a 1:1 ratio of cobaloxime precursor $Co(dmgH)(dmgH_2)Cl_2$ and the corresponding pyridyl-functionalized BODIPYs (**B1-B4**) in the presence of TEA in a mixture of methanol and dichloromethane at room temperature, as shown in Scheme 1. A more detailed description of the synthesis and the analytical characterization is given in the Experimental Section. The desired products were precipitated and isolated by filtration. Axial coordination of BODIPY units (**B1-B4**) to the $Co(dmgH)(dmgH_2)Cl_2$ was characterized by the changes observed in the aromatic region of the ^1H NMR spectra with all NMR signals undergoing an up-field shift. These BODIPY-sensitized cobaloximes in the solid state can be stored in the dark for a long time without decomposition.

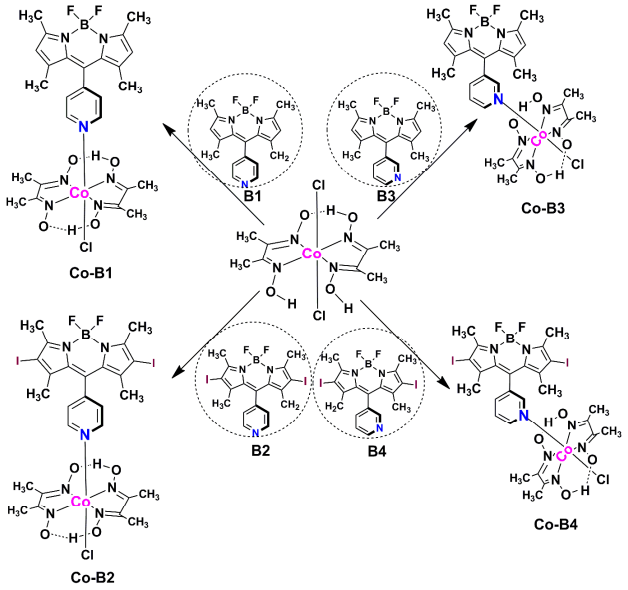

Scheme 1. Synthesis of BODIPY cobaloximes **Co-Bn** (n = 1-4).

2.2. Solid-state structure analysis

Well-formed X-ray-quality single crystals of pyridine-substituted BODIPY derivatives (**B1-B3**) except **B4** were obtained by slow evaporation of their CH_2Cl_2 solution**.** As shown in Figure 1, the single crystal X-ray diffractions reveal there are two isomers of both **B1** and **B3** in their respective asymmetric unit cells, while the asymmetric unit of **B2** only

contains one independent molecule. The crystallographic details are shown in Table S1(ESI†). As expected, in each BODIPY unit, the central six-membered ring lies coplanar with the two adjacent five-membered rings. The rms deviation from planarity is 0.012 Å for **B1** (the average of 0.010 and 0.014 Å in two molecules), 0.0 Å for **B2**, and 0.012 Å for **B3** (the average of 0.010 and 0.014 Å in two molecules), respectively, indicating the nearly planar degree of C_9BN_2 frame for **B1**-**B3**. The dihedral angle between the *meso*-pyridine and BODIPY moiety is 84.3º in **B1** (the average of 87.45 and 81.15º in two molecules) and 82.77º in **3** (the average of 83.40 and 82.14º in two molecules), indicating an almost perpendicular configuration between the *meso*-pyridine and BODIPY moiety for **B1** and **B3**. In contrast, the *meso*-pyridine ring is completely orthogonal to the indacene plane with dihedral angle of 90º in **B2**.

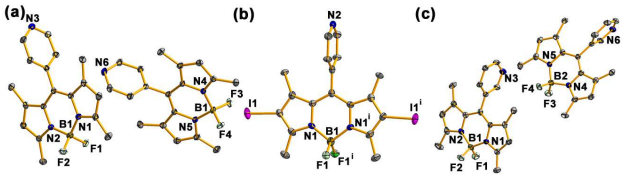

Figure 1. ORTEP diagram of pyridine-substituted BODIPY derivatives **B1** (a), **B2** (b) and **B3** (c). Symmetry code: (i) –x, y, -z+1/2. Thermal ellipsoids drawn at the 50% probability level. H atoms omitted for clarity.

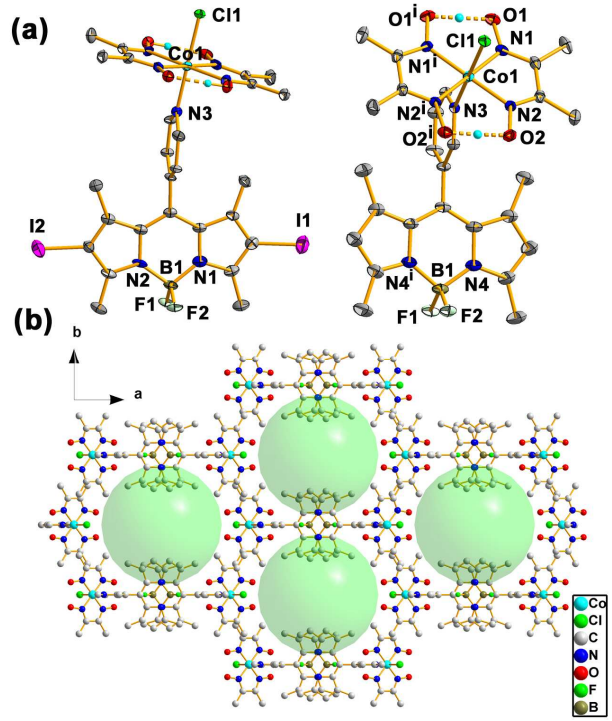

Figure 2. (a) Solid-state molecular structures of **Co-B2** (left) found in the unit cell of **Co-B2**·2CH_3CN and **Co-B3** (right). Symmetry code: (i) x, -y+1, z; Thermal ellipsoids displaying 50% probability level. Solvent molecules and hydrogen atoms (except bridging hydrogen atoms of the cobaloxime macrocycle) are omitted for clarity. (b) Crystal packing of **Co-B3** when viewed in the [001] direction.

Structural characterization and the stereochemistry of BODIPY-cobaloxime complexes (**Co-B1**, **Co-B2**, and **Co-B3**) except **Co-B4** were further confirmed through X-ray crystallography (Figure 2). The crystallographic data are given in Table S2 (ESI†). In **Co-B1** and **Co-B2**, the refined structure reveals a six-coordinate Co(III) ion that is ligated by two coplanar dimethylglyoximate ligands and trans chloride and pyridine ligands. The observed axial Co-$N_{pyridine}$ distances of 1.952 Å in **Co-B1**, and 1.955 Å in **Co-B2** agree closely with those of in other Co(III) cobaloximate complexes, such as $Co(dmgH)_2pyCl$ with a Co-$N_{pyridine}$ distance of 1.959 Å.[16]

A crystallographic study on the molecular device **Co-B3** suggested that **Co-B3** crystallized in the C2/m space group, which contemplates a mirror plane bisecting the BODIPY and cobaloxime (Figure 2a). **Co-B3** shows the expected distorted octahedral coordination geometry with a *meta*-pyridyl and a chloride ligand in the axial location and a pair of dmgH ligands joined in the equatorial plane through intramolecular hydrogen bonds between the oxime oxygen atoms [O1···O1^i, 2.486(3) Å; O2···O2^i, 2.472(3) Å]. The average Co-N_{imine} and Co-$N_{pyridine}$ bond distances in **Co-B3** are 1.897 and 1.958 Å, respectively, and do not significantly differ from those found in **Co-B1** or **Co-B2**. The most interesting features of the crystal structure are revealed by the analysis of the packing diagram. Firstly, two adjacent molecules pack via weak B-F···π and π···π interactions to generate a molecular dimer. Secondly, the neighboring dimers are involved in additional nonclassic H-bonds (C_{methyl}-H···Cl) interactions generating a two-dimensional (2D) sheet structure (Figure 2b). When 2D networks are viewed in the [001] direction, it is revealed that these interactions lead to the formation of rhombic channels. The rhombic channels of ca. ~11.4 × 6.2 Å contain no guest solvent molecules. The amount of void space encapsulated the network is 912.5 Å^3, i.e., 25% of the unit cell volume.

2.3. Photophysical properties and electrochemical studies

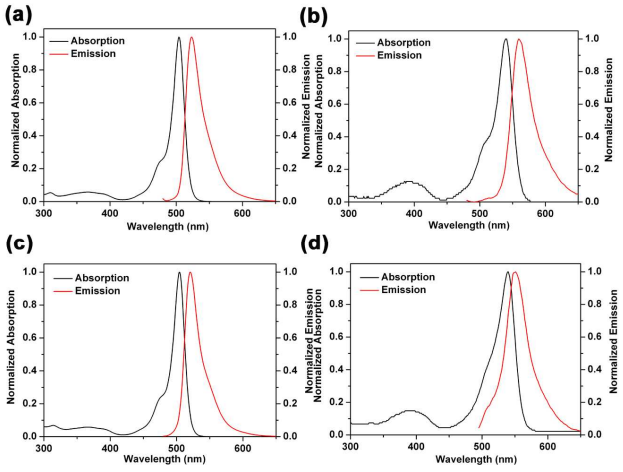

Figure 3. Absorbance and emission spectra of BODIPY dyes: (a) **B1**, (b) **B2**, (c) **B3**, and (d) **B4**. $c = 1.0 \times 10^{-5}$ M in CH_3CN, at room temperature.

A series of BODIPY derivatives (**B1**-**B4**) were characterized via UV-vis absorption and fluorescence spectroscopy in various solvents with increasing polarity from toluene to methanol, and photophysical parameters are gathered in Table 1. It should be

noteworthy that some photophysical data for **B2** in dichloromethane and acetonitrile is previously reported.[14] As shown in Figure 3, **B1** and **B3** share a similar absorption and emission profile with high extinction coefficients (ε = 79700 for **B1** and 78200 for **B3**) and high quantum efficiency of fluorescence (Φ_{fl} = 0.82 for **B1** and 0.76 for **B3**), irrespective of *para*- or *meta*-pyridyl substitution. It is noteworthy that the previously measured Φ_{fl} for **B1** in CH_2Cl_2 is only 0.30.[14] However, both we and S. Banfi[15b] have determined the Φ_{fl} of **B1** in CH_2Cl_2 is ~0.70-0.80. Upon iodination of two pyrrole 2,6-positions, both the absorption and emission maxima of **B2** and **B4** shift to lower energy. The absorption coefficients of bis-iodo-BODIPYs **B2** and **B4** are comparable to those of nonhalogenated BODIPYs **B1** and **B3**; however the Φ_{fl} of both **B2** and **B4** sharply decreases to 0.01-0.02 in CH_3CN. Significant decrease of Φ_{fl} is an indication of an efficient intersystem crossing efficiency (Φ_{isc}) from the lowest singlet excited state (S_1) to one of the other triplet states except the lowest one (T_1), which has been accelerated by the internal heavy-atom effect.[15a]

Table 1 Photophysical parameters of **B1-B4** in different solvents.

BODIPY	solvent	absorption		fluorescence		
		λ_{max}[a](nm)	ε[b](M^{-1} cm^{-1})	λ_{em}[c](nm)	Φ_{fl}[d](%)	τ[e](ns)
B1	$PhCH_3$	507	88200	519	0.80	2.06
	CH_2Cl_2	504	80500	514	0.71	2.00
	THF	504	80400	516	0.60	1.89
	CH_3CN	500	79700	512	0.82	1.92
	CH_3OH	502	84700	514	0.46	1.44
B2	$PhCH_3$	542	57700	555	0.03	*f*
	CH_2Cl_2	541	62300	557	0.02	*f*
	THF	538	52300	558	0.02	*f*
	CH_3CN	534	52200	561	0.01	*f*
	CH_3OH	538	50000	556	0.01	*f*
B3	$PhCH_3$	507	88500	517	0.79	2.96
	CH_2Cl_2	505	87400	514	0.66	2.94
	THF	505	79700	514	0.77	2.73
	CH_3CN	501	78200	511	0.76	3.05
	CH_3OH	502	85200	514	0.54	2.66
B4	$PhCH_3$	542	66400	554	0.03	*f*
	CH_2Cl_2	540	63400	554	0.02	*f*
	THF	539	55000	560	0.02	*f*
	CH_3CN	534	58800	551	0.02	*f*
	CH_3OH	537	65600	559	0.02	*f*

[a]λ_{max} (nm): absorption wavelength (at the maximum intensity). [b]ε (M^{-1} cm^{-1}): extinction coefficient. [c]λ_{em} (nm): emission wavelength (at the maximum intensity). [d]Φ_{fl} (%): the fluorescence quantum yields of **B1** and **B3** were estimated with 1,3,5,7-tetramethyl-8-phenyl-BODIPY as a standard (Φ_{fl} = 0.72 in tetrahydrofuran); the fluorescence quantum yields of **B2** and **B4** were estimated with Rhodamine B (0.49 in ethanol). [e]τ (ns): fluorescence lifetimes. [f]Not determined.

The frontier molecular orbital (FMO) diagrams were also generated for the BODIPYs (**B1-B4**) from the optimized geometries. Time-dependent density functional theory (TDDFT) calculations in combination with the 6-31+G(d) basis set and a solvation model for acetonitrile were performed to determine the transitions involved in the lowest energy states. The parameters for the optimized geometries and full list of excited states are included in the Electronic Supplementary Information. Both **B1** and **B3** possess a highest occupied molecular orbital (HOMO) that is of BODIPY π character and a lowest unoccupied molecular orbital (LUMO) that is a BODIPY-based π^* orbital. The TDDFT calculation shows a lowest energy singlet transition of HOMO→LUMO character with a high oscillator strength of 0.58 and energy of 2.86 eV. Although the energy of the predicted BODIPY-based transition is much higher than that of the observed experimental values, TDDFT calculations are known to overestimate the excitation energy of BODIPY chromophores.[12,17] The **B2** and **B4** were hypothesized to enable the formation of the triplet excited state by ISC as iodine atoms are introduced into the cores of BODIPYs. The HOMO(π)-LUMO(π^*) transition corresponds to the first singlet excitation as assigned by TDDFT, which is observed in other BODIPY derivatives.[13] In each iodinated BODIPY, the nature of the HOMO and LUMO is unchanged upon iodization (see ESI†). The computed similarity between these FMO orbitals indicates that, apart from its influence on the rate of ISC, iodination exerts negligible change on the electronic structures of the BODIPYs.

The optical properties of these BODIPY-sensitized cobaloximes **Co-Bn** (n = 1-4) were examined by electronic absorption spectroscopy at room temperature (Figure S1 of ESI†). Figure 4 shows the absorption spectra of these complexes as well as the reference $Co(dmgH)_2pyCl$ and reagent $Co(dmgH)(dmgH_2)Cl_2$ in CH_3CN. These studied complexes exhibit a combination of absorption features from their specific subunits of BODIPYs and cobaloximes, indicating they absorb light efficiently throughout the ultraviolet and visible regions. The visible region is dominated by intense peak more than 500 nm, which corresponds to the 0-0 vibrational band of the $S_0 \rightarrow S_1$ ($\pi \rightarrow \pi^*$) transition localized on the BODIPY chromophore. Complexation of BODIPYs with cobaloxime leads to a bathochromic shift of the BODIPY absorption maxima of 5 nm. Two strong high-energy absorption bands at ~230 and ~255 nm were assignable to spin-allowed intraligand ($\pi \rightarrow \pi^*$) transitions of the dmgH ligand from cobaloxime. It can be noted that the absorption spectra of these complexes are largely superpositions of their individual subunits: this indicates that the interactions between the cobaloxime and BODIPY chromophores in the ground state are weak and complexation of the BODIPY to the cobaloxime causes minimal perturbation of its optical properties, so that these complexes can be regarded as supramolecular systems.

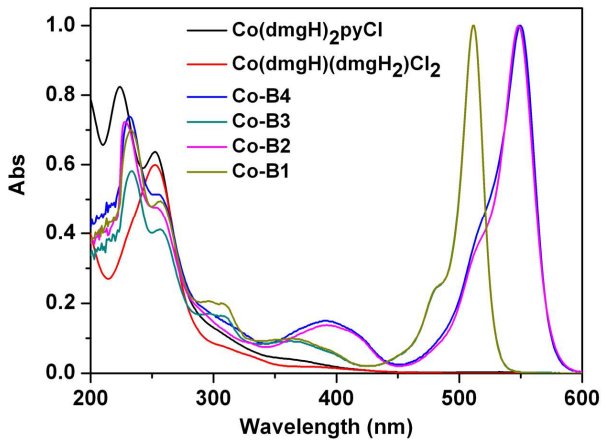

Figure 4. Absorption spectra of BODIPY-sensitized cobaloximes **Co-Bn** (n = 1-4). $c = 1.0 \times 10^{-5}$ M in CH_3CN, at room temperature.

The steady-state fluorescence studies were further carried out on these supramolecular systems (Figure S2 of ESI†). Attachment of the cobaloximes is accompanied by a substantial decrease in fluorescence from the BODIPY chromophore due to intramolecular energy or electron transfer across the orthogonal structure. Since we will observe photocatalytic hydrogen production for these supramolecular systems, these observations supported the hypothesis that the quenching of BODIPY-based fluorescence was due to the intramolecular electron-transfer processes in which the cobaloxime serves as an acceptor.

The electrochemical activity of the BODIPY dyes **B1-B4** and the above-prepared complexes **Co-Bn** (n = 1-4) was determined by cyclic voltammetry in dichloromethane using tetrabutylammonium hexafluorophosphate (TBAP) as a supporting electrolyte, and the results are gathered in Table 2. BODIPYs with two iodo atoms on the *β*-positions (**B2** and **B4**) have more positive reduction and oxidation potentials than non-iodinating BODIPYs (**B1** and **B3**), which is consistent with previously reported results (Table 2).[15] The oxidation and reduction potentials of *para*-pyridyl attached at the 8-position of BODIPY are similar to and *meta*-pyridyl substituted BODIPYs, demonstrating that the position of *meso*-pyridyl substitutions has little electron effect on the redox activity of the central BODIPY core. This tendency is consistent with the aforementioned results by optical analysis. When pyridyl-functionalization BODIPYs are bound to the cobaloximes, the redox potentials were found to occur at more positive values. The catalytically relevant Co^{III}/Co^{II} redox couple is of special interest for hydrogen evolution, and can be assigned, together with the reference complex $Co(dmgH)_2pyCl$ for comparison. In the noniodinated BODIPY-cobaloximes **Co-B1** and **Co-B3**, the Co^{III}/Co^{II} redox couple is slightly reduced, by 0.06 V (**Co-B1**) and 0.05 (**Co-B3**). However, for the iodinated complexes, the potential of the Co^{III}/Co^{II} redox couple is significantly reduced, by 0.22 V (**Co-B2**) and 0.26 V (**Co-B4**), when compared to the reference $Co(dmgH)_2pyCl$. Through these comparisons, it was clear that this substantial reduction in the reduction potential of the Co^{III}/Co^{II} redox couple for **Co-B2** and **Co-B4** is a favourable step toward photogeneration of hydrogen.

Table 2 Electrochemical redox data for the BODIPY derivatives **B1-B4** and BODIPY-cobaloximes **Co-Bn** (n = 1-4) as well as the reference $Co(dmgH)_2pyCl$.[a]

Compound	$E_{1/2ox}$, V	$E_{1/2red}$, V
B1	0.76, 0.95	-1.58
B2	0.93, 1.10	-1.34
B3	0.75, 0.98	-1.58
B4	0.91, 1.13	-1.36
Co-B1	1.01	-0.95, -1.72
Co-B2	0.79, 1.02	-0.79, -1.17, -1.42
Co-B3	1.02	-0.96, -1.68
Co-B4	0.83, 1.02	-0.75, -1.05, -1.36
$Co(dmgH)_2pyCl$	0.74	-1.01

[a]Potentials determined by cyclic voltammetry in deoxygenated CH_2Cl_2 solution, containing 0.1 M TBAP as the supporting electrolyte, at a solute concentration of *ca*. 1.0 mM and at room temperature. Potentials were standardized versus ferrocene (F_c) as internal reference.

2.4. Photocatalytic hydrogen evolution

To optimize H_2 photocatalysis experiments for these BODIPY-cobaloximes, we initially used 2,6-diiodo BODIPY-sensitized cobaloxime **Co-B4** as the model of photocatalyst with TEOA as sacrificial electron donor using a Xe lamp (300 W) with a cutoff filter ($\lambda > 420$ nm). No significant reaction is observed in the dark in the presence of the photocatalyst or without TEOA under light irradiation. We investigated the medium effects on photocatalytic hydrogen production of **Co-B4**. Among the solvents tested, CH_3CN-H_2O, DMF-H_2O, THF-H_2O, CH_3OH-H_2O, CH_3CH_2OH-H_2O (3:2, v/v), the best result for photoinduced H_2 generation with **Co-B4** (1.1×10^{-4} M) and TEOA (5%, v/v) was obtained in CH_3CN-H_2O (3:2, v/v), with 9 TON of H_2 evolution (Figure 5). The solvent dependence for hydrogen production from this system probably may be ascribed to many factors including solvent polarity, stabilization of reduction intermediates and Co(II/I) reduction potential necessary for hydrogen generation.[18,19] The optimal ratio for CH_3CN and water was further investigated. Changing the ratio of CH_3CN-H_2O from 3:2 to 1:1 resulted in considerable decrease in H_2 evolution to 2 TON. However, increasing the CH_3CN/H_2O ratio to 4:1 and then to 24:1, while keeping the catalyst concentration constant at 1.1×10^{-4} M, notably increases the activity of the catalyst, as indicated by consistently higher TON values. Indeed, the TON values as high as 19 and 74 have been, respectively, obtained and, these correspond to volumes of hydrogen of 4.6 and 18 mL. Similar effects of the ratios of CH_3CN-H_2O on the photoinduced H_2 production with the $Pt^{II}PS/Co^{III}$ catalyst systems were previously reported by Eisenberg.[18] The explanation for the apparent effect of the content of water may result from changes in the electrostatic properties of the medium and differences in the redox potentials as the CH_3CN-H_2O ratio changes.[9] Several other possible sacrificial electron donors such as triethylamine (TEA), ascorbate and EDTA were tried, but TEOA proved to be the most effective at hydrogen production under the same reaction conditions. The potential electron donors of TEA and ascorbate

only achieve TON 1 and 8, respectively, while EDTA resulted in no hydrogen production.

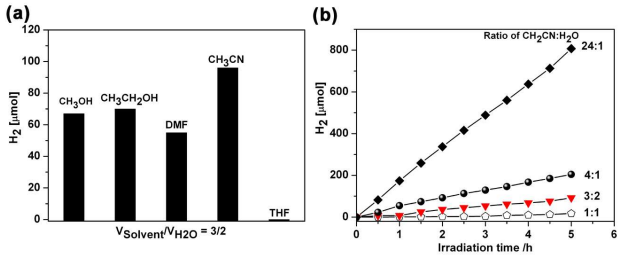

Figure 5. (a) Comparison of hydrogen production using different solvent:water (3:2, v/v) with 1.1×10^{-4} M **Co-B4**, TEOA (5%, v/v). (b) Comparison of hydrogen production using different ratios of CH_3CN/H_2O with 1.1×10^{-4} M **Co-B4**, TEOA (5%, v/v).

The hydrogen evolving performance of **Co-B4** was found to be strongly dependent on pH, with results in terms of TONs peaking at the value of 8.5. As displayed in Figure 6, the TON based on complex **Co-B4** was 85 (935 μmol) in a TEOA (5% v/v) and CH_3CN/water (4:1) with pH = 8.5 after 5 h irradiation. The rate of H_2 production decreases sharply at both more acidic and more basic values. This strong dependence of the rate of H_2 evolution on pH has been observed in related photocatalytic system.[10b,19] The pH-dependence is likely to arise from a balance between several factors playing together towards hydrogen generation: (i) the protonation of TEOA diminishing its ability to function as an electron donor with decreasing pH, (ii) the proton concentration and thermodynamic driving-force for water reduction (lower at basic pH than at acidic one), (iii) the formation of the cobalt hydride catalytic intermediate which is much more favored at acidic pH, and (iv) the presence of competition for protonation or metal coordination of BODIPY at more acidic medium.

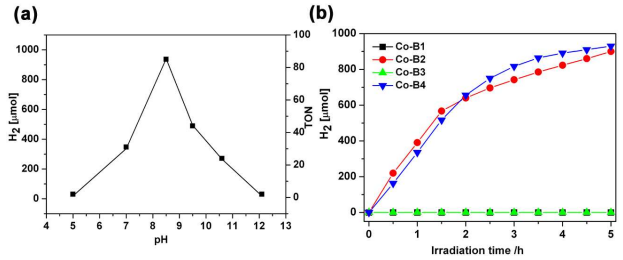

Figure 6. (a) Influence of the pH on the photocatalytic H_2 evolution from a system comprising **Co-B4** (1.1×10^{-4} M) and TEOA (5%, v/v) in CH_3CN/H_2O (4:1, v/v). (b) Comparision of hydrogen production using different BODIPY-cobaloximes **Co-Bn** (n = 1-4) with c = 1.1×10^{-4} M, TEOA (5%, v/v) in CH_3CN/H_2O (4:1, v/v) at pH 8.5.

To compare the efficiency of **Co-B4** to those of **Co-Bn** (n = 1-3), these catalysts were tested under the same experimental conditions with 100 mL of CH_3CN/H_2O (4:1, v/v) containing 1.1×10^{-4} M **Co-Bn** (n = 1-4), TEOA (5%, v/v) combined in a 250 mL Pyrex flat-bottomed flask vigorously agitated with a magnetic stirrer. The pH of reaction system was kept at 8.5 with a 2.5 M HCl stock solution. Under these optimized conditions, as shown in Figure 6, the changes in the iodinated and noniodinated BODIPYs of **Co-Bn** (n = 1-4) result in quite different performances of H_2 generation. The H_2 evolution levels off after 5 h irradiation, with the turnovers of H_2 evolved up to 85 (935 umol) for **Co-B4** under optimal conditions, while **Co-B2** gave 82 turnovers (900 umol) of H_2 evolution in 5 h irradiation and no amount of H_2 production was detected by GC for **Co-B1** and **Co-B3**. Compared with iodinated **Co-B2** and **Co-B4**, noniodinated **Co-B1** and **Co-B3** lack any appreciable hydrogen evolution under the same reaction conditions due to the absence of internal heavy atom effect and long-lived photoexcited triplet state. In fact, previous studies have suggested that the heavy atom effect of the iodine substituents facilitates ISC to the longer-liver $^3\pi\pi^*$ excited state from which electron transfer occurred. The **Co-B4** displays much higher photocatalytic efficiency than that reported for the photocatalyst composed of a Ru-based (TON = 14)[20] or porphyrin chromophore (TON = 22) and the same Co^{III} cobaloxime with a similar pyridyl coordination linkage.[9] It should be noteworthy that the irradiation wavelength chosen substantially affects the hydrogen evolving efficiency. When we used purposely a 550±10 nm excitation (green monochromatic light) to ensure excitation near the absorption maxima of iodinated BODIPY, only 6 and 7 of TON was obtained for **Co-B2** and **Co-B4**.

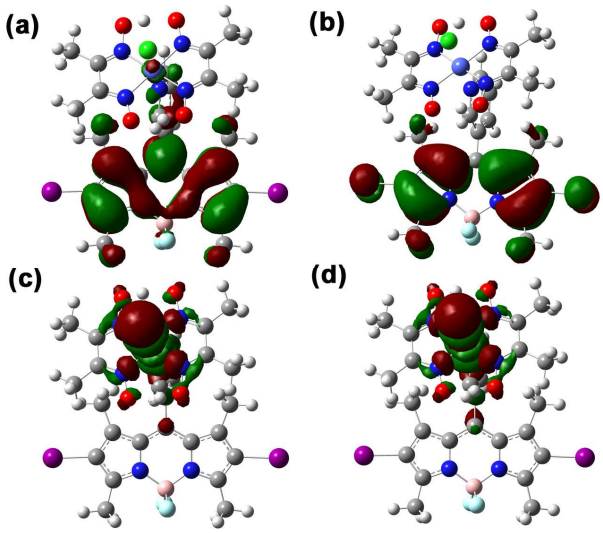

Figure 7. Frontier molecular orbitals of **Co-B4**$^-$ obtained through DFT calculations (UB3LYP/LANL2DZ) since the anion has an unpaired electron. The alpha/beta molecular orbitals were all defined due to the negative charge the open-shell system adopted. Both the HOMO orbitals of alpha (a) and beta (b) are exclusively localized on the BODIPY chromophores, while the LUMO orbitals of alpha (c) and beta (d) are located on the cobalt centers.

The redox potentials of **Co-B2** and **Co-B4** are adopted to evaluate the driving force of the intramolecular electron transfer reaction. According to the reduction potentials of **Co-B2** and **Co-B4**, the ground-state redox potentials of **B2** ($E_{1/2}$ (**B2**$^{+}$/**B2** = 1.02 V and $E_{1/2}$(**B2**$^{-}$/**B2**) = -1.42 V) and **B4** ($E_{1/2}$ (**B4**$^{+}$/**B4** = 1.02 V and $E_{1/2}$(**B4**$^{-}$/**B4**) = -1.36 V), and the triplet excited state energies of ^{3}**B2*** (1.513 eV) and ^{3}**B4*** (1.514 eV) obtained from TDDFT calculations, the free energy ΔG for formation of the Co^I species can be estimated according to the well-known Rehm-Weller equation (Table S4, ESI†).[21] The calculated ΔG suggests that the reduction process is exergonic, and intramolecular electron transfer from reduced **Bn**$^-$(n = 2 and 4)

species to the cobaloximes is thermodynamically feasible for **Co-B2** and **Co-B4**, as estimated from the electrochemical and spectroscopic data.

For additional information on the location of the frontier molecular orbitals, we examined **Co-B2**$^{\cdot-}$ and **Co-B4**$^{\cdot-}$ by means of the density functional theory (DFT) methods on the UB3LYP/LANL2DZ level. Geometric parameters from the X-ray diffraction and analysis were used for the calculations. As expected, orthogonalization of the BODIPY moieties and cobaloximes results in the frontier molecular orbital residing on the individual units. Contributions to the HOMO distribution were mainly from the BODIPY chromophores, while the LUMO distributions were donated by all atomic orbitals in the centre of cobalt, as displayed in Figure 7. Therefore, the transition of HOMO→LUMO is a full electron-transfer process (from π-conjugated BODIPY$^{\cdot-}$ radical anion to cobaloxime fragment), which is in accordance with the experimental results.

Drawing on previous studies for the mechanisms of hydrogen evolution by cobaloxime catalysts[10,12] and the results described above, it is postulated that the key step involves the generation of a catalytically active Co^{I} species. As shown in Scheme 2, there is one possible pathway for the generation of Co^{I} species with the quenching of the triplet BODIPY excited state (denoted $^{3}BDP^{*}$): *i.e.*, reductive quenching mechanism by electron transfer from TEOA, whereupon the BDP$^{\cdot-}$ species formed transfers an electron to Co^{II}. The path produces the radical cation of TEOA$^{\cdot+}$, which decomposes through proton loss, electron transfer and hydrolysis to form glycolaldehyde and di(ethanol)amine along with transfer of a second proton and a second electron. The formed Co^{I} species further reacts with a proton to produce a postulated Co^{III}-hydride, which releases molecular hydrogen via a homo-or heterolytic pathway.[22]

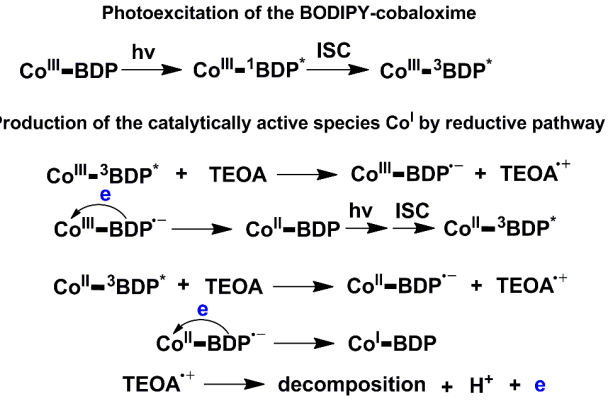

Scheme 2. Plausible mechanism for the formation of Co^{I} species. TEOA stands for triethanolamine and BDP for iodinated BODIPYs **B2** and **B4.**

3. Conclusions

In conclusion, we report four noble-metal-free supramolecular systems **Co-Bn** (n =1-4) with pyridine atoms of BODIPY moieties binding to the Co^{III} center of cobaloxime, and use them as single-component homogeneous photocatalytsts for visible-light-driven H_2 evolution. Many factors including the medium, sacrificial electron donor, the ratio of solvent/water and pH in the reaction medium, irradiation wavelength are carefully investigated. Under optimized conditions (relative low photocatalyst concentration of 110 μmol L^{-1}, at weak basic pH ~8.5, CH_3CN/water ratio of 4:1, irradiation wavelength λ > 420 nm), the TONs of hydrogen evolution for iodinated **Co-B2** and **Co-B4** are 85 and 82, respectively, while the noniodinated **Co-B1** and **Co-B3** show no photocatalytic activity under the same reaction conditions. This study demonstrates unambiguously the beneficial effects for H_2 production of the use of such a photocatalyst in which the iodine heavy atoms are attached onto the BODIPY cores. This internal heavy atom effect stabilizes the system and enables the efficient formation of the long-lived triplet excited state photosensitizers by ISC, which is vital for the production of hydrogen. A reductive quenching pathway (namely, the intramolecular electron transfers from BDP$^{\cdot-}$ to the cobalt centers) in the photochemically driven step is possible for the hydrogen production, as evaluated by from the electrochemical and photophysical data as well as theoretical calculations. To our knowledge, the photoinduced H_2-evolving efficiency of **Co-B4** up to 21 mL is the highest one ever reported for the absolutely precious-metal-free supramolecular photocatalysts.

4. Experimental section

4.1. Chemicals and Instrumentation

Reagents were purchased as reagent-grade and used without further purification unless otherwise stated. Solvents were dried by standard literature methods[23] before being distilled and stored under nitrogen over 3Å molecular sieves prior to use. All reactions were performed under a nitrogen atmosphere in oven-dried or flame-dried glassware unless otherwise stated and were monitored by TLC using 0.25 mm silica gel plates with UV indicator (60F-254).

^{1}H and ^{13}C NMR were obtained at room temperature using a Bruker PLUS 400 spectrometer with tetramethylsilane (TMS, 0.00 ppm) as an internal standard and $CDCl_3$ as solvent. Chemical shift multiplicities are reported as s = singlet, d = doublet, and br = broad singlet. Coupling constants (*J*) values are given in Hz. Mass spectrometry (MS) experiment was carried out in the positive ion made on a Bruker Esquire HCT ion trap mass spectrometer (Billerica, MA) coupled with a homemade electrospray ionization (ESI) device. Parameters of the ESI source were optimized to enhance the signal intensity. The pressure of nebulizing nitrogen, the flow rate of desolvation gas, and the temperature of desolvation gas were set to 8 psi, 1L min^{-1}, and 250 ºC, respectively. Cyclic voltammetry experiments were carried out with a CHI 650E electrochemical analyzer using a three-electrode system at room temperature. The working electrode was 2 mm Pt with a Pt wire as auxiliary electrode and a 0.01M $Ag/AgNO_3$ solution reference electrode. All measurements were performed in freshly distilled and deoxygenated dichloromethane with a solute concentrate of ca. 1.0 mM in the presence of 0.1 M tetrabutylammonium hexafluorophosphate (TBAP) as a supporting electrolyte. C, H,

and N microanalyses were carried out with a CE instruments EA 1110 analyzer.

4.2. Spectroscopic Measurements and Determination of Fluorescent Life and Quantum Yields

The solvents used for photophysical measurement were of spectroscopic grade and used without further purification. UV-vis spectra in solution were recorded on a UV-2100 (Shimadzu) spectrophotometer. Steady-state fluorescence spectroscopic studies in solution were performed on a Hitachi F-7000 spectrophotometer with a xenon arc lamp as light source. The slit width was set at 2.5 nm for excitation and 5.0 nm for emission. Fluorescence decay curves of the samples were measured with the time-correlated single-photon-counting (TCSPC) method on FLSP920 Lifespec-ps (Edinburgh) and the data were analyzed by Edinburgh software. The goodness of the fit of the decays as judged by reduced chi-squared (χ^2_R) and autocorrelation function $C(j)$ of the residuals was below $\chi^2_R < 1.1$. The fluorescence decay time (τ) was obtained from the slope. Samples for absorption and emission measurements were contained in 1 cm × 1 cm quartz cuvettes. Measurements were made using optically dilute solutions after deoxygenation by purging with dried N_2.

Relative quantum efficiencies of fluorescence of BODIPY derivatives were obtained by comparing the area under the corrected emission spectrum of the test sample with 8-phenyl-4,4-difluoro-1,3,5,7-tetramethyl 4-bora-3a,4a-diaza-*s*-indacene (0.72 in tetrahydrofuran)[24] and Rhodamine B (0.49 in ethanol)[25] as standards, respectively. Dilute solutions ($0.01 < A < 0.05$) were used to minimize the reabsorption effects. The following equation was used to calculate quantum yield:[26]

$$\Phi_{fl}^{sample} = \Phi_{fl}^{standard} \times (I^{sample}/I^{standard}) \times (A^{standard}/A^{sample}) \times (n^{sample}/n^{standard})^2$$

Where Φ_{fl}^{sample} and $\Phi_{fl}^{standard}$ are the emission quantum yields of the sample and the reference, respectively, $A^{standard}$ and A^{sample} are the measured absorbances of the reference and sample at the excitation wavelength, respectively, $I^{standard}$ and I^{sample} are the area under the emission spectra of the reference and sample, respectively, and $n^{standard}$ and n^{sample} are the refractive indices of the solvents of the reference and sample, respectively. The Φ_{fl}^{sample} values reported in this work are the averages of multiple (generally three), fully independent measurements.

4.3. Synthetic Procedures

The syntheses of the starting BODIPY compounds **B1** and **B2** were achieved using literature methods[15] and characterized by ^{1}H NMR, ^{13}C NMR and elemental analyses to determine their structures.

4,4-difluoro-8-(4-pyridyl)-1,3,5,7-tetramethyl-4-bora-3a,4a-diaza-*s*-indacene (B1): In a flame-dried Schlenk flask, under nitrogen atmosphere, to a stirred solution of 2,4-dimethyl-pyrrole (0.62 mL, 6 mmol) and 4-pyridylcarbaldehyde (0.28 mL, 3 mmol) in anhydrous CH_2Cl_2 (150 mL) were added trifluoroacetic acid (TFA, 0.15 mL). The solution was stirred overnight at room temperature in the dark until TLC indicated complete consumption of the aldehyde. Dichlorodicyanobenzoquinone (DDQ, 681 mg, 3 mmol) were added and the mixture was stirred for an additional 2h. A large excess of triethylamine (9 mL) and $BF_3{\cdot}Et_2O$ (9 mL) was then added into the reaction mixture. After being stirred for 12 h at room temperature, it was diluted with water and extracted with CH_2Cl_2. The organic layer was combined, dried over $MgSO_4$ and evaporated to dryness under vacuum. The crude product was purified by chromatography on a column packed with flash silica gel, using CH_2Cl_2 as eluent, from which the desired product **B1** was obtained as orange solid in 15.3% (155 mg). ^{1}H NMR ($CDCl_3$, 400 MHz): δ (ppm) = 8.80 (d, J = 3.4 Hz, 2H), 7.34 (d, J = 2.6 Hz, 2H), 6.02 (s, 2H), 2.56 (s, 6H), 1.41 (s, 6H). ^{13}C NMR ($CDCl_3$, 101 MHz): δ (ppm) = 156.44, 150.53, 143.60, 142.62, 137.60, 130.29, 123.31, 121.79, 14.57. Anal. Cacld for $C_{18}H_{18}BF_2N_3$: C, 66.49; H, 5.58; N, 12.92. Found: C, 66.42; H, 5.51; N, 12.85. ESI-MS m/z ($C_{18}H_{18}BF_2N_3$) calculated: 325.2, found 326.1 ($M+H^+$), 348.1 ($M+Na^+$).

4,4-difluoro-8-(4-pyridyl)-1,3,5,7-tetramethyl-2,6-diiodo-4-bora-3a,4a-diaza-*s*-indacene (B2): To **B1** (127.5 mg, 0.39 mmol) in 10 mL of CH_3CH_2OH was added iodine (198.9 mg, 0.78 mmol) and iodic acid (149.0 mg, 0.84 mmol). This mixture was left stirring at room temperature for 24 h, washed with an aqueous solution of sodium carbonate, and extracted by CH_2Cl_2. Organic layers were combined, dried over Na_2SO_4, and evaporated to dryness under vacuum. Purification was performed by column chromatography on silica gel using CH_2Cl_2 as eluent to obtain the desired product **B2** as purple solid in 78% (176.4mg). ^{1}H NMR ($CDCl_3$, 400 MHz): δ (ppm) = 8.88 (s, 2H), 7.52 (d, J = 9.8 Hz, 2H), 2.67 (s, 6H), 1.42 (s, 6H). ^{13}C NMR ($CDCl_3$, 101 MHz): δ (ppm) = 158.06, 150.19, 144.71, 144.22, 136.62, 130.12, 123.57, 86.43, 17.31, 16.15. Anal. Cacld for $C_{18}H_{16}BF_2I_2N_3$: C, 37.47; H, 2.80; N, 7.28. Found: C, 37.60; H, 2.91; N, 7.41. ESI-MS m/z ($C_{18}H_{16}BF_2I_2N_3$) calculated: 577.0, found 576.1 ($M-H^+$).

4,4-difluoro-8-(3-pyridyl)-1,3,5,7-tetramethyl-4-bora-3a,4a-diaza-*s*-indacene (B3): In a flame-dried Schlenk flask, under nitrogen atmosphere, to a stirred solution of 2,4-dimethyl-pyrrole (0.41 mL, 4 mmol) and 3-pyridylcarbaldehyde (0.19 mL, 2 mmol) in anhydrous CH_2Cl_2 (100 mL) were added trifluoroacetic acid (TFA, 0.1 mL). The solution was stirred overnight at room temperature in the dark until TLC indicated complete consumption of the aldehyde. Dichlorodicyanobenzoquinone (DDQ, 454 mg, 2 mmol) were added and the mixture was stirred for an additional 2h. A large excess of triethylamine (6 mL) and $BF_3{\cdot}Et_2O$ (6 mL) was then added into the reaction mixture. After being stirred for 12 h at room temperature, it was diluted with water and extracted with CH_2Cl_2. The organic layer was combined, dried over $MgSO_4$ and evaporated to dryness under vacuum. The crude product was purified by chromatography on a column packed with flash silica gel, using CH_2Cl_2 as eluent, from which the desired product **B1** was obtained as orange solid in 11.3% (76 mg). ^{1}H NMR ($CDCl_3$, 400 MHz): δ (ppm) = 8.78 (d, J = 4.31, 1H); 8.59 (s, 1H), 7.70 (dd, J = 1.79, 1.57, 1H), 7.51(dd, J = 4.92, 4.92, 1H), 6.00(s, 2H), 2.57(s, 6H), 1.38(s, 6H).^{13}C NMR ($CDCl_3$, 400 MHz): δ (ppm) = 156.50, 149.68, 148.02, 142.70, 136.61, 136.82, 136.58, 131.56, 123.94, 121.86, 15.02, 14.65. Anal. Cacld for $C_{18}H_{18}BF_2N_3$: C, 66.49; H, 5.58; N, 12.92. Found: C, 66.55; H, 5.48; N, 12.99. ESI-MS m/z ($C_{18}H_{18}BF_2N_3$) calculated: 325.2, found 326.2 ($M+H^+$).

4,4-difluoro-8-(3-pyridyl)-1,3,5,7-tetramethyl-2,6-diiodo-4-bora-3a,4a-diaza-*s*-indacene (B4): To **B3** (114.3 mg, 0.35 mmol) in 10 mL of CH_3CH_2OH was added iodine (184.4 mg, 0.72 mmol) and iodic acid (134.6 mg, 0.76 mmol). This mixture was left stirring at room temperature for 24 h, washed with an aqueous solution of sodium carbonate, and extracted by CH_2Cl_2. Organic layers were combined, dried over Na_2SO_4, and evaporated to dryness under vacuum. Purification was performed by column chromatography on silica gel using CH_2Cl_2 as eluent to obtain the desired product **B4** as purple solid in 81.2% (164.7 mg). ^{1}H NMR($CDCl_3$, 400 MHz): δ (ppm) = 8.84 (dd, J = 1.44, 1.54, 1H), 8.57 (d, J = 1.85, 1H), 7.67 (dd, J = 1.61, 1.55, 1H), 7.54 (m, J = 4.71, 1H), 2.67(s, 6H), 1.42(s, 6H). ^{13}C NMR ($CDCl_3$, 400 MHz): δ (ppm) = 157.74, 150.62, 148.22, 144.93, 136.83, 135.91, 131.36, 131.20, 123.92, 86.28, 17.57, 16.11. Anal. Cacld for $C_{18}H_{16}BF_2I_2N_3$: C, 37.47; H, 2.80; N, 7.28. Found: C, 37.57; H, 2.88; N, 7.45. ESI-MS *m/z* ($C_{18}H_{16}BF_2I_2N_3$) calculated: 577.0, found 576.1 (M-H$^+$).

A modified literature procedure was followed for synthesis of BODIPY-cobaloxime complexes (**Co-B1** and **Co-B2**). The reagent $Co(dmgH)(dmgH_2)Cl_2$ and reference pyridine-cobaloxime $Co(dmgH)_2pyCl$ were prepared according to the literature methods.[27,28]

[{Co(dmgH)$_2$Cl}{4,4-difluoro-8-(4-pyridyl)-1,3,5,7-tetramethyl-4-bora-3a,4a-diaza-*s*-indacene}] (Co-B1): To a stirred solution of $Co(dmgH)(dmgH_2)Cl_2$ (43.6 mg, 0.123 mmol) in anhydrous CH_3OH (5 mL) was added triethylamine (Et_3N, 16.9 uL, 0.12 mmol). The solution slowly turned into yellow-brown in color. **B1** (39.2 mg, 0.12 mmol) in CH_2Cl_2 (3 mL) was then added. The reaction mixture was stirred for 3 h at room temperature. The formed microcrystalline purple precipitate was filtered off and washed with small amounts of ice cold CH_3OH until the filtrate had no residual fluorescence under UV illumination. After drying under high vacuum, a dark purple product was obtained (yield 65.7mg, 81.3%). ^{1}H NMR ($CDCl_3$, 400 MHz,): δ (ppm) = 8.47 (d, J = 6.6 Hz, 2H), 7.29(s,1H), 7.28 (s, 1H), 6.01 (s, 2H), 2.55 (s, 6H), 2.45 (s, 12H), 1.17 (s, 6H). ^{13}C NMR ($CDCl_3$, 101 MHz): δ (ppm) = 157.73, 152.63, 151.90, 147.24, 134.25, 129.59, 125.48, 122.46, 14.69, 14.10, 13.05. UV-vis, λ_{max}/nm, (ε/L mol^{-1} cm^{-1}), (CH_3CN): 233 nm (53900), 257 nm (38200), 361 nm (7600), 505 nm (77000).

[{Co(dmgH)$_2$Cl}{4,4-difluoro-8-(4-pyridyl)-1,3,5,7-tetramethyl-2,6-diiodo-4-bora-3a,4a-diaza-*s*-indacene}] (Co-B2): To a stirred solution of $Co(dmgH)(dmgH_2)Cl_2$ (26.1 mg, 0.074 mmol) in anhydrous CH_3OH (5 mL) was added triethylamine (Et_3N, 10.1 uL, 0.072 mmol). The solution slowly turned into yellow-brown in color. **B1** (40.2 mg, 0.07 mmol) in CH_2Cl_2 (3 mL) was then added. The reaction mixture was stirred for 3 h at room temperature. The formed microcrystalline purple precipitate was filtered off and washed with small amounts of ice cold CH_3OH until the filtrate had no residual fluorescence under UV illumination. After drying under high vacuum, a dark purple product was obtained (yield 54.4 mg, 87%). ^{1}H NMR ($CDCl_3$, 400 MHz): δ (ppm) = 8.50 (d, J = 5.8 Hz, 2H), 7.33 (d, J = 5.1 Hz, 2H), 2.65 (s, 6H), 2.53 (s, 12H), 1.21 (s, 6H). UV-vis, λ_{max}/nm, (ε/L mol^{-1} cm^{-1}), (CH_3CN): 228 nm (45600), 251 nm (30000), 389 nm (8600), 540 nm (63000).

[{Co(dmgH)$_2$Cl}{4,4-difluoro-8-(3-pyridyl)-1,3,5,7-tetramethyl-4-bora-3a,4a-diaza-*s*-indacene}] (Co-B3): To a stirred solution of $Co(dmgH)(dmgH_2)Cl_2$ (77 mg, 0.22 mmol) in anhydrous CH_3OH (5 mL) was added triethylamine (Et_3N, 29.8 uL, 0.21 mmol). The solution slowly turned into yellow-brown in color. **B3** (69.5 mg, 0.21 mmol) in CH_2Cl_2 (3 mL) was then added. The reaction mixture was stirred for 3 h at room temperature. The formed microcrystalline purple precipitate was filtered off and washed with small amounts of ice cold CH_3OH until the filtrate had no residual fluorescence under UV illumination. After drying under high vacuum, a dark purple product was obtained (yield 120.5 mg, 82.2%). ^{1}H NMR ($CDCl_3$, 400 MHz) δ (ppm) = 8.43 (d, J = 5.60, 1H), 8.28(s, 1H), 7.68(d, J = 7.45, 1H), 7.42(m, J = 6.23, 1H), 6.02(s, 2H), 2.58(s, 6H), 2.41(s, 12H), 1.06(s, 6H). ^{13}C NMR ($CDCl_3$, 400 MHz): δ (ppm) = 157.71, 152.49, 151.17, 150.12, 141.19, 139.24, 133.47, 131.01, 125.90, 122.36, 14.72, 14.22, 12.97. UV-vis, λ_{max}/nm, (ε/L mol^{-1} cm^{-1}), (CH_3CN): 232 nm (44200), 256 nm (31300), 361 nm (7010), 506 nm (76000).

[{Co(dmgH)$_2$Cl}{4,4-difluoro-8-(3-pyridyl)-1,3,5,7-tetramethyl-2,6-diiodo-4-bora-3a,4a-diaza-*s*-indacene}] (Co-B4): To a stirred solution of $Co(dmgH)(dmgH_2)Cl_2$ (30 mg, 0.085 mmol) in anhydrous CH_3OH (5 mL) was added triethylamine (Et_3N, 11.4 uL, 0.081 mmol). The solution slowly turned into yellow-brown in color. **B1** (47.3 mg, 0.085 mmol) in CH_2Cl_2 (3 mL) was then added. The reaction mixture was stirred for 3 h at room temperature. The formed microcrystalline purple precipitate was filtered off and washed with small amounts of ice cold CH_3OH until the filtrate had no residual fluorescence under UV illumination. After drying under high vacuum, a dark purple product was obtained (yield 66.6 mg, 90.1%). ^{1}H NMR ($CDCl_3$, 400 MHz): δ (ppm) = 8.49 (d, J = 6.0 Hz, 2H), 2.62 (s, 6H), 2.46 (s, 12H), 1.17 (s, 6H). UV-vis, λ_{max}/nm, (ε/L mol^{-1} cm^{-1}), (CH_3CN): 231 nm (40000), 250 nm (27700), 389 nm (8110), 542 nm (54000).

4.4. Crystallization Experiments and X-ray Crystallography

Well-formed X-ray-quality crystals of **B1**, **B2** and **B3** were obtained by slow evaporation of their CH_2Cl_2 solution at room temperature. Suitable crystals of **Co-B1** and **Co-B2** were grown by slow evaporation of solutions in CH_2Cl_2/CH_3CN 3:1, and **Co-B3** were grown by the slow evaporation of a solution in toluene/DMF 1:1.

Intensity data for these compounds were collected on a Rigaku R-AXIS RAPID Image Plate single-crystal diffractometer using graphite-monochromated Mo Kα radiation source (λ = 0.71073 Å). Single crystals of these compounds with appropriate dimensions were chosen under an optical microscope, coated in oil and mounted on a glass fiber for data collection. Absorption correction was applied by correction of symmetry-equivalent reflections using the ABSCOR program.[29] All structures were solved by direct methods using SHELXS-97[30] and refined by full-matrix least-squares on F^2 using SHELXL-97[31] via the program interface X-Seed.[32] Non-hydrogen atoms were refined anisotropically. Hydrogen atoms attached to oxygen in **Co-B1, Co-B2** and **Co-B3** were located by difference Fourier maps and other hydrogen atoms were isotropically in a riding model with U_{iso} values 1.2-1.5 times

those of their parent atoms. All structures were examined using the Addsym subroutine PLATON[33] to ensure that no additional symmetry could be applied to the models. Crystal structure views were obtained using Diamond v3.1.[34] Details of the data collection conditions and the parameters of the refinement process are given in Table S1 and Table S2. Selected bond lengths and angles are listed in Table S3.

4.5. Water splitting reaction

The photocatalytic water splitting experiment was performed in a Pyrex top-irradiation reaction vessel connected to a glass closed gas circulation system (Labsolar-IIIAG photocatalytic system, Beijing Perfectlight Co., Ltd., Figure S3). In a typical hydrogen production experiment, 1.1×10^{-4} M solutions of the BODIPY-cobaloximes **Co-Bn** (n = 1-4) were prepared in a mixture of acetonitrile-water 4:1 (v/v), containing 5 vol% of triethanolamine (TEOA) at pH = 8.5. The obtained reactant solution was put into a 250 mL Pyrex flat-bottomed reaction vessel and vigorously stirred in the dark for 0.5 h. The reaction system was evacuated three times with half an hour each time to remove air completely prior to visible light illumination. The reaction solution was irradiated using an external light source comprising a 300 W Xe arc lamp (MICROSOLAR 300, Beijing Perfectlight Co., Ltd.) with an optical filter employed to cut off light with wavelengths below 420 nm. During the water photochemical reaction, the reaction mixture was mixed using a magnetic stirring bar and the temperature of the reactant solution was maintained at room temperature by a flow of cooling water. The amount of H_2 gas produced in the reaction system was measured with a gas chromatograph (GC 7900, Shanghai Techcomp Instrument Ltd.) with a thermal conductivity detector (TCD), a 5 Å molecular sieve column (4 mm(OD) × 3mm(ID) × 3m), and with N_2 as carrying gas. Each photocatalysis experiment was conducted three times with the reported μmol hydrogen being the average of the trials. The amounts of hydrogen were quantified by external standard method, and the turnovers were calculated versus the amount of BODIPY-cobaloxime in the systems.

4.6. Computational Details

Theoretical calculations have been performed with the *Gaussian 09* software package.[35] The geometric parameters from X-ray diffraction analysis were used as the starting point for the geometry optimization when available. Geometries were optimized under the DFT level of theory using the hybrid functional B3LYP, which combines Becke's 3-parameter exchange functional[36] and Lee, Yang, and Parr's correlation functional.[37] The polarizable continuum model (PCM)[38] of acetonitrile was used in all calculations. The BODIPY chromophores were optimized using the 6-31+G(d) basis set,[39] excluding the iodinated compound, for which 3-21G[40] was used for iodine while the 6-31+G(d) was used for the remaining atoms. For the optimization of BODIPY-cobaloximes, LAN2DZ[41] basis set on the Co atoms, 3-21G basis set on the iodine and 6-31+G(d) basis set for the rest were used. All geometries were deemed minima, as no negative frequencies were found. TDDFT[42] was used to model the excitation energies. All molecular orbitals were visualized with the software *GaussView* 5.0.

Acknowledgements

The National Natural Science Foundation of China (no. 21201066) funded this research. Financial support from the Natural Science Foundation of Fujian Province (no. 2011J01047), the outstanding Youth Scientific Research Cultivation Plan of Colleges and Universities of Fujian Province (JA13008), and Promotion Program for Young and Middle-aged Teacher in Science and Technology Research of Huaqiao University (ZQN-PY104) are also greatly acknowledged. We thank the anonymous reviewers for their constructive suggestions in improving this manuscript.

Notes and references

(1) (a) K. Sakai and H. Ozawa, *Coord. Chem. Rev*., 2007, **251**, 2753-2766; (b) S. Berardi, S. Drouet, L. Francàs, C. Gimbert-Suriñach, M. Guttentag, C. Richmond, T. Stoll and A. Llobet, *Chem. Soc. Rev*., 2014, doi: 10.1039/c3cs60405e.

(2) (a) A. Kudo and Y. Miseki, *Chem. Soc. Rev*., 2009, **38**, 253; (b) M. G. Walter, E. L. Warren, J. R. Mckon, S. W. Boettcher, Q. Mi, E. A. Santori and N. S. Lewis, *Chem. Rev*., 2010, **110**, 6446; (c) T. Hisatomi, J. Kubota and K. Domen, *Chem. Soc. Rev*., 2014, doi: 10.1039/c3cs60378d; (d) J. R. Ran, J. Zhang, J. G. Yu, M. Jaroniec and S. Z. Qiao, *Chem. Soc. Rev*., 2014, doi: 10.1039/c3cs60425j.

(3) T. S. Teets and D. G. Nocera, *Chem. Commun*., 2011, **47**, 9268-9274.

(4) (a) M. Wang, Y. Na, M. Gorlov and L. C. Sun, *Dalton Trans*., 2009, 6458-6467; (b) W. T. Eckenhoff and R. Eisenberg, *Dalton Trans*., 2012, **41**, 13004-13021.

(5) H. Ozawa, M. Haga and K. Sakai, *J. Am. Chem. Soc*., 2006, **128**, 4926-4927; (b) H. Ozawa, M. Kobayashi, B. Balan, S. Masaoka and K. Sakai, *Chem.-Asian J*., 2010, **5**, 1860-1869.

(6) S. Rau, B. Schäfer, D. Gleich, E. Anders, M. Rudolph, M. Fredrich, H. Görls, W. Henry and J. G. Vos, *Angew. Chem., Int. Ed*., 2006, **45**, 6215-6218.

(7) (a) M. Elvington, J. Brown, S. M. Arachchige and K. J. Brewer, *J. Am. Chem. Soc*., 2007, **129**, 10644-10645; (b) K. Rangan, S. M. Arachchige, J. R. Brown and K. J. Brewer, *Energy Environ. Sci*., 2009, **2**, 410-419.

(8) S. Jasimuddin, T. Yamada, K. Fukuju, J. Otsuki and K. Sakai, *Chem. Comm*., 2010, **46**, 8466-8468.

(9) P. Zhang, M. Wang, C. X. Li, X. Q. Li, J. F. Dong and L. C. Sun, *Chem. Commun*., 2010, **46**, 8806-8808.

(10) (a) P. Zhang, M. Wang, J. F. Dong, X. Q. Li, F. Wang, L. Z. Wu and L. C. Sun, *J. Phys. Chem. C*, 2010, **114**, 15868-15874; (b) T. Lazarides, T. McCormick, P. W. Du, G. G. Luo, B. Lindley and R. Eisenberg, *J. Am. Chem. Soc*., 2009, **131**, 9192-9194; (c) T. M. McCormick, B. D. Calitree, A. Orchard, N. D. Kraut, F. V. Bright, M. R. Detty and R. Eisenberg, *J. Am. Chem. Soc*., 2010, **132**, 15480-15483.

(11) A. Loudet and K. Burgess, *Chem. Rev*., 2007, 107, 4891-4932.

(12) R. P. Sabatini, T. M. McCormick, T. Lazarides, K. C. Wilson, R. Eisenberg and D. W. McCamant, *J. Phys. Chem. Lett*., 2011, **2**, 223-227.

(13) (a) Z. H. Pan, J. W. Zhou and G. G. Luo, *Phys. Chem. Chem. Phys*., 2014, **16**, 16290-16301; (b) Z. H. Pan, G. G. Luo, J. W. Zhou, J. X. Xia, K. Fang and R. B. Wu, *Dalton Trans*., 2014, **43**, 8499-8507; (c) G. G. Luo, J. X. Xia, K. Fang, Q. H. Zhao, J. H. Wu and J. C. Dai, *Dalton Trans*., 2013, **42**, 16268-16271.

(14) J. Bartelmess, A. J. Francis, K. A. EI Roz, F. N. Castellano, W. W. Weare and R. D. Sommer, *Inorg. Chem*., 2014, **53**, 4527-4534.

(15) (a) T. Yogo, Y. Urano, Y. Ishitsuka, F. Maniwa and T. Nagano, *J. Am. Chem. Soc*., 2005, **127**, 12162-12163; (b) E. Caruso, S. Banfi,

P. Barbieri, B. Leva and V. T. Orlandi, *J. Photochem. Photobiol. B: Biol*., 2012, **114**, 44-51.
(16) S. Geremía, R. Dreos, L. Randaccio and G. Tauzher, *Inorg. Chim. Acta*, 1994, **216**, 125-129.
(17) (a) R. Nithya, P. Kolandaivel and K. Senthilkumar, *Mol. Phys*., 2012, **110**, 445-456; (b) J. B. Prieto, F. L. Arbeloa, V. M. Martinez, T. A. Lopez and I. L. Arbeloa, *Phys. Chem. Chem. Phys*., 2004, **6**, 4247-4253; (c) D. Jacquemin, S. Chibani, B. L. Guennic and B. Mennucci, *J. Phys. Chem. A* 2014, **118**, 5343-5348; (d) S. Chibani, A. D. Laurent, B. L. Guennic and D. Jacquemin, *J. Chem. Theory Comput*., 2014, DOI: 10.1021/ct500655k.
(18) L. M. Utschig, S. C. Silver, K. L. Mulfort and D. M. Tiede, *J. Am. Chem. Soc*., 2011, **133**, 16334-16337.
(19) P. W. Du, J. Schneider, G. G. Luo, W. W. Brennessel and R. Eisenberg, *Inorg. Chem*., 2009, **48**, 4952-4962.
(20) A. Fihri, V. Artero, M. Razavet, C. Baffert, W. Leibl and M. Fontecave, *Angew. Chem., Int. Ed*., 2008, **47**, 564-567.
(21) D. Rehm and A. Weller, *Ber. Bunsenges. Phys. Chem*., 1969, **73**, 834-839.
(22) J. L. Dempsey, B. S. Brunschwig, J. R. Winkler and H. B. Gray, *Acc. Chem. Res*., 2009, **42**, 1995-2004.
(23) J. A. Riddick, W. B. Bunger and T. K. Sakano, *Organic Solvents*, 4th ed.; Wiley-Interscience, New York, 1986.
(24) Y. C. Wang, D. K. Zhang, H. Zhou, J. L. Ding, Q. Chen, Y. Xiao and S. X. Qian, *J. Appl. Phys*., 2010, *108*, 455-462.
(25) K. G. Casey and E. L. Quitevis, *J. Phys. Chem*., 1988, **92**, 6590.
(26) J. R. Lakowicz, *Principles of Fluorescence Spectroscopy*, 3rd ed.; Springer: New York, 2006.
(27) G. N. Schrauzer, *Inorg. Synth*., 1968, **11**, 61.
(28) W. C. Trogler, R. C. Stewart, L. A. Epps and L. G. Marzilli, *Inorg. Chem*., 1974, **13**, 1564-1570.
(29) T. Higashi, *ABSCOR*, Empirical Absorption Correction based on Fourier series Approximation; Rigaku Corporation: Tokyo, 1995.
(30) G. M. Sheldrick, *SHELXS-97*, Program for X-ray Crystal Structure Determination; University of Gottingen: Germany, 1997.
(31) G. M. Sheldrick, *SHELXL-97*, Program for X-ray Crystal Structure Refinement; University of Gottingen: Germany, 1997.
(32) L. J. Barbour, X-Seed, A software tool for Supramolecular Crystallography; *Supramol. Chem*. 2001, **1**, 189-191.
(33) A. L. Spek, Implemented as the *PLATON* Procedure, a Multi-purpose Crystallographic Tool; Utrecht University: Utrecht, The Netherlands, 1998.
(34) K. Brandenburg, *DIAMON*D, Version 3.1f; Crystal Impact GbR: Bonn, Germany, 2008.
(35) M. J. Frisch, G. W. Trucks, H. B. Schlegel, G. E. Scuseria, M. A. Robb, J. R. Cheeseman, G. Scalmani, V. Barone, B. Mennucci, G. A. Petersson, H. Nakatsuji, M. Caricato, X. Li, H. P. Hratchian, A. F. Izmaylov, J. Bloino, G. Zheng, J. L. Sonnenberg, M. Hada, M. Ehara, K. Toyota, R. Fukuda, J. Hasegawa, M. Ishida, T. Nakajima, Y. Honda, O. Kitao, H. Nakai, T. Vreven, J. A. Montgomery Jr,., J. E. Peralta, F. Ogaliaro, M. Bearpark, J. J. Heyd, E. Brothers, K. N. Kudin, V. N. Staroverov, R. Kobayashi, J. Normand, K. Raghavachari, A. Rendell, J. C. Burant, S. S. Iyengar, J. Tomasi, M. Cossi, N. Rega, J. M. Millam, M. Klene, J. E. Knox, J. B. Cross, V. Bakken, C. Adamo, J. Jaramillo, R. Gomperts, R. E. Stratmann, O. Yazyev, A. J. Austin, R. Cammi, C. Pomelli, J. W. Ochterski, R. L. Martin, K. Morokuma, V. G. Zakrzewski, G. A. Voth, P. Salvador, J. J. Dannenberg, S. Dapprich, A. D. Daniels, O. Farkas, J. B. Foresman, J. V. Ortiz, J. Cioslowski and D. J. Fox, *Gaussian*, Inc., Wallingford CT., 2009.
(36) A. D. Becke, *J. Chem. Phys*., 1993, **98**, 5648-5652.
(37) C. Lee, W. Yang and R. G. Parr, *Phys. Rev. B*., 1988, **37**, 785-789.
(38) E. Cances, B. Mennucci and J. Tomasi, *J. Chem. Phys*., 1997, **107**, 3032-3041.
(39) A. D. Becke, *J. Chem. Phys*., 1993, **98**, 1372-1377.
(40) A. D. Becke, *J. Chem. Phys*., 1998, **109**, 2092-2098.
(41) M. Dolg, U. Wedig, H. Stoll and H. Press, *J. Chem. Phys*., 1987, **86**, 866-872.
(42) M. Rudolph and J. Autschbach, *J. Chem. Phys*., 2010, **132**, 184103-184109.

Graphical Abstract

Four BODIPY-cobaloxime systems **Co-Bn** (n = 1-4) were studied as single-component homogeneous photocatalytic systems for H_2 generation in aqueous media.